



Article

Conducting Polymer Metallic Emerald: Magnetic Measurements of Nanocarbons/Polyaniline and Preparation of Plastic Composites

Yusuke Koshikawa ¹, Ryo Miyashita ¹, Takuya Yonehara ¹, Kyoka Komaba ¹, Reiji Kumai ²  and Hiromasa Goto ^{1,*} 

¹ Department of Materials Science, Faculty of Pure and Applied Sciences, University of Tsukuba, Tsukuba 305-8573, Ibaraki, Japan

² Photon Factory, Institute of Materials Structure Science (IMSS), High Energy Accelerator Research Organization (KEK), Tsukuba 305-0801, Ibaraki, Japan

* Correspondence: gotoh@ims.tsukuba.ac.jp

Abstract: Synthesis of polyaniline in the presence of fullerene nanotubes (nanocarbons) in water was carried out with oxidative polymerization. The surface of the sample showed metallic emerald green color in bulk like the brilliance of encrusted gemstones. The composite showed unique magnetic behavior, such as microwave power-dependent magnetic resonance as magnetic spin behavior and macroscopic paramagnetism with a maximum χ value at room temperature evaluated with superconductor interference device. Surface structure of the composite was observed with optical microscopy, circular polarized differential interference contrast optical microscopy, scanning electron microscopy, and electron probe micro analyzer. Polymer blends consisting of polyaniline, nano-carbons, and hydroxypropylcellulose or acryl resin with both conducting polymer and carbon characters were prepared, which can be applied for electrical conducting plastics. The combination of conducting polymer and nano-carbon materials can produce new electro-magneto-active soft materials by forming a composite. This paper reports evaluation of magnetic properties as a new point of nanocarbon and conducting polymer composite.

Keywords: conductive polymer; fullerene; polyaniline; magnetism



Citation: Koshikawa, Y.; Miyashita, R.; Yonehara, T.; Komaba, K.; Kumai, R.; Goto, H. Conducting Polymer Metallic Emerald: Magnetic Measurements of Nanocarbons/Polyaniline and Preparation of Plastic Composites. *C* **2022**, *8*, 60. <https://doi.org/10.3390/c8040060>

Academic Editor: Manuel Fernando Ribeiro Pereira

Received: 28 September 2022

Accepted: 1 November 2022

Published: 4 November 2022

Publisher's Note: MDPI stays neutral with regard to jurisdictional claims in published maps and institutional affiliations.



Copyright: © 2022 by the authors. Licensee MDPI, Basel, Switzerland. This article is an open access article distributed under the terms and conditions of the Creative Commons Attribution (CC BY) license (<https://creativecommons.org/licenses/by/4.0/>).

1. Introduction

Nanocarbon has been studied from both fundamental aspects and applications in new technologies. Especially, carbon peapods are a product of nanotechnology and an interesting carbon-based material in which spherical fullerenes exist in tubular carbon [1]. The carbon peapods containing fullerene exhibit characteristic physical behavior, such as the movement of fullerenes inside the carbon tubes and electronic interactions between the carbon nanotubes and fullerenes [2–8].

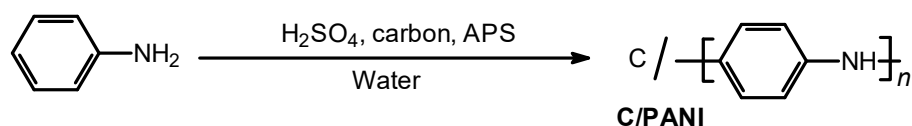
Since the discovery of polyacetylene films with a metallic reflection, conducting polymers have been developed and applied in a research field of plastic electronics. π -Conjugated polymers, as a precursor for conducting polymers before doping, have been applied in electroluminescent devices, solar cells, and sensors. General π -conjugated polymers can be synthesized in organic solvents using the following coupling polycondensation reactions: Migita–Kosugi–Stille coupling, Mizoroki–Heck reaction to prepare polyarylene-vinylene, Negishi coupling reaction, and direct arylation method recently developed by Kanbara [9,10] using a Pd complex catalyst. The Sonogashira–Hagihara reaction can prepare conjugated polymers with triple bonds using Cu and Pd complex catalysts. Ni-based catalysts can be used to prepare conjugated polymers using the Kumada–Tamao–Corriu coupling reaction [11]. A Ta-based catalyst is useful for preparation of polyacetylene derivatives [12]. Electrochemical polymerization in chiral liquid crystal can be prepared electro-optically active polymers [13].

Polyaniline (PANI) is one of the representative conducting polymers. The electrical conduction mechanism and synthesis method of PANI are unique in conjugated polymers. The conductivity of PANI can be explained by a combination of π -electron-based electrical conduction via the movement of polarons (radical cations) and bipolarons (dications) upon doping and ionic conduction support. The production of PANI is environmentally friendly because the synthesis of PANI has been performed in a water medium. In addition, the aniline monomer has been used as a raw material of dyes and is inexpensive and readily available.

In this report, a composite of fullerene nanocarbons and PANI is prepared by the polymerization of aniline in the presence of the nanocarbons. The polymerization reaction occurred on the surface of the nanocarbon reaction field. The resulting PANI is grown and adhered to the surface to form a carbon/PANI composite. We report the synthesis of the composites showing metallic structural color and the magnetic property for the development of conducting polymer and nanocarbon science.

2. Synthesis

Aniline was polymerized in the presence of carbons in water using ammonium peroxydisulfate (APS) as an oxidant for this synthesis. A solution of nanocarbons 5 mL (4 g/L water solution, tubes@rice, fullerene nanotubes), 1.020 g of aniline as a monomer, 1.032 g of sulfuric acid, and 0.993 g of APS in water was stirred at 0 °C. After 24 h, the solution was filtered and washed with a large volume of methanol, followed by drying in vacuum to obtain 0.114 g of a powders of metallic emerald green color in bulk like the brilliance of encrusted gemstones. The resulting product is abbreviated as C/PANI. Scheme 1 presents the synthesis of C/PANI.



Scheme 1. Preparation of the C/PANI composite. APS: Ammonium peroxydisulfate. PANI: Polyaniline. Carbon: Fullerene nanotubes.

3. Results

3.1. Fourier Transform Infrared

Figure 1 shows the Fourier transform infrared (FT-IR) absorption spectrum of C/PANI. MacDiarmid et al. reported various doping states of PANI [14]. The characteristic absorptions of PANI, the C=C stretching vibrations due to the quinonoid structure (Q) and benzenoid structure (B) (Figure 2), were observed at 1561 cm^{-1} and 1491 cm^{-1} , respectively, due to the Q-B-Q sequence structure. The as-prepared PANI fraction was doped by H_2SO_4 during polymerization. The doped PANI consisted of benzenoid and quinonoid units at the molecular level. The C=N stretching vibration due to the Q-B-Q structure was observed at 1298 cm^{-1} , and the CN stretching vibration due to the B-B-B structure was exhibited at 1243 cm^{-1} . Thus, PANI could be synthesized in the presence of the carbons. The absorption of the carbons in the composite overlapped with the benzenoid structure of PANI. In addition, the PANI signal occupied the entire absorption caused by the surface of the carbons being covered with the PANI layer.

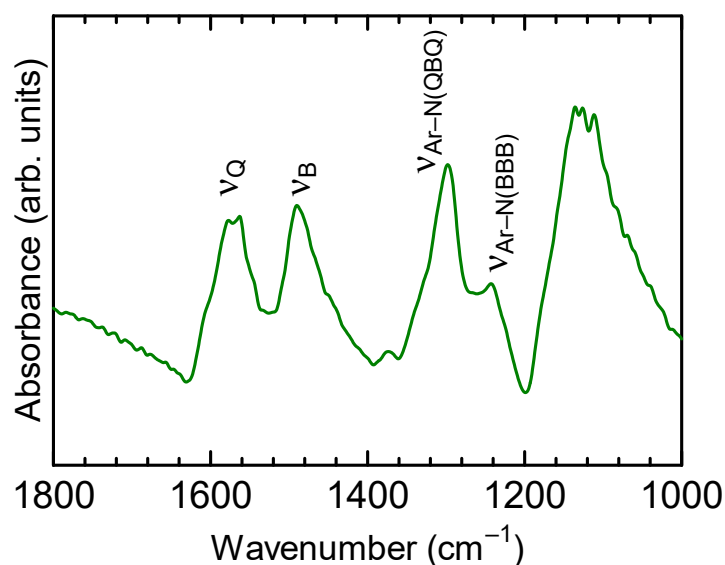


Figure 1. Fourier transform infrared spectrum of C/PANI.

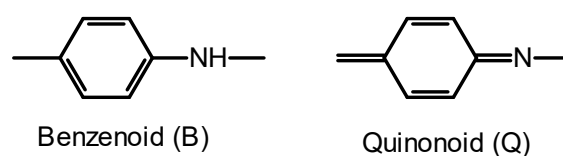


Figure 2. Benzenoid (B) and quinonoid (Q) units in PANI.

3.2. Ultraviolet-Visible

Figure 3 shows the Ultraviolet-visible (UV-vis) absorption spectrum of the C/PANI dissolved in *N*-methyl pyrrolidone (NMP). The absorption band due to the π - π^* transition of the main chain of polyaniline was observed at 324 nm. The absorption band originating from a polaron as a doping band appeared at 629 nm. The spectral shape can be emeraldine base as a half-doped form of soluble fraction in NMP. The absorption band of the pristine PANI was observed at 637 nm in the previous study [15]. The blue shift of the C/PANI may be related to interaction between PANI and the carbons [16].

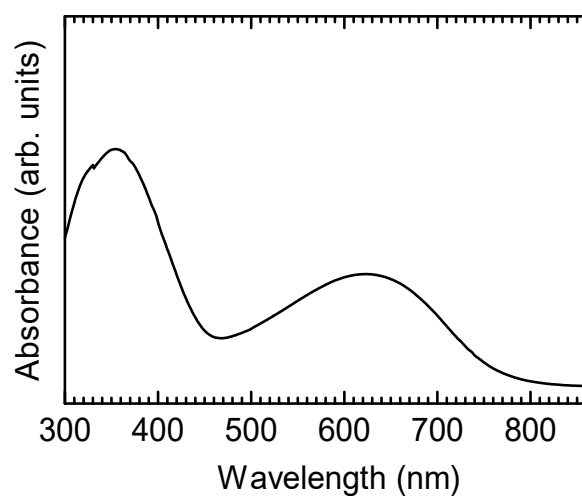


Figure 3. Ultraviolet-visible optical absorption spectrum of C/PANI in *N*-methyl pyrrolidone solution.

3.3. Surface Image

Appearance of sample images after filtration in the purification process of the C/PANI is displayed in Figure 4, showing the brilliance of encrusted gemstones. Figure 4a shows

a magnified image of a metallic purple part of the sample. Figure 4b,c show further magnification of the metallic emerald green part. The C/PANI displays various reflection colors, such as emerald green, purple, bronze, and metallic emerald green. This may be due to the fact that the as-prepared C/PANI is a doped form with free electrons. Interaction between carbon and PANI can increase electron mobility in the bulk for showing plasma reflection like polyacetylene. Further, dispersion of the nanocarbon component in the C/PANI composite may exhibit structural color. The combination of the plasma like reflection and sample structural color with intrinsic color of the doped PANI element resulted metallic emerald color, as a form of metallic emeraldine of PANI. Previously, PANI has been defined as the emeraldine forms. The present research realized a metallic color emeraldine in bulk.

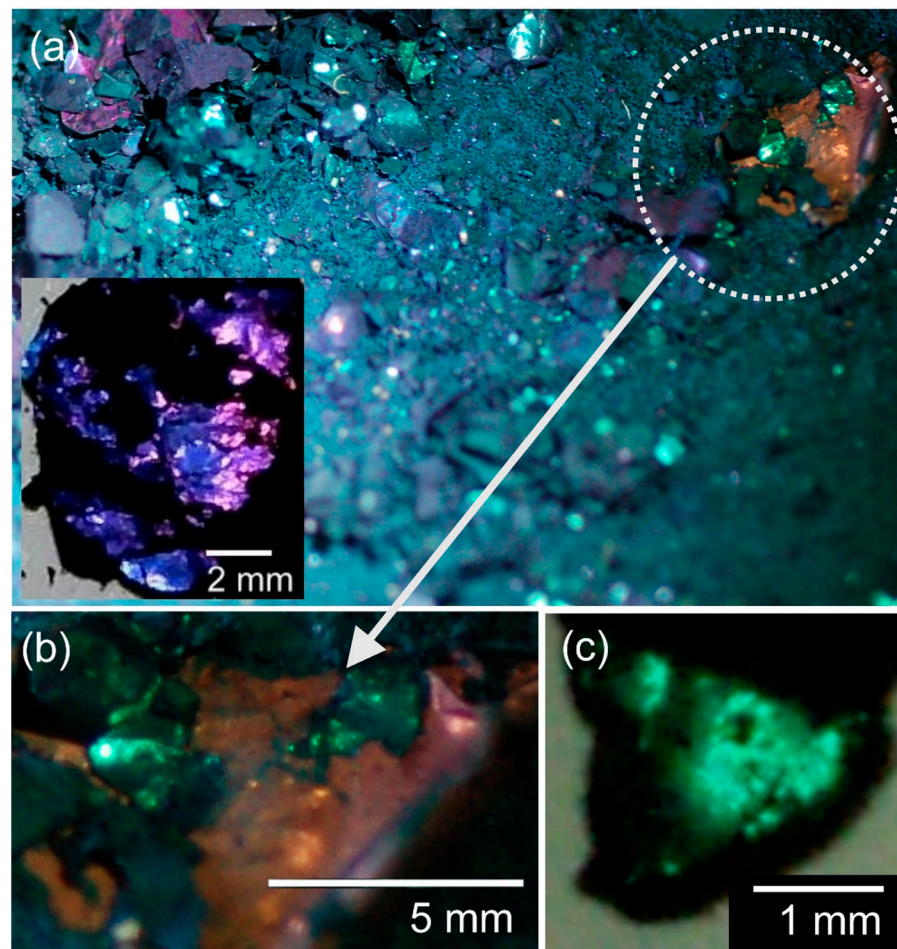


Figure 4. Appearance of C/PANI. (a) Surface image of C/PANI after filtration in the purification. (b,c) Magnifications of the metallic emeraldine part.

Figure 5 shows a circular polarized differential interference contrast optical microscopy (C-DIM) image of the metallic emeraldine part of the C/PANI sample, showing a colorful surface. The surface color can be due to metallic reflection and structural color of the C/PANI.

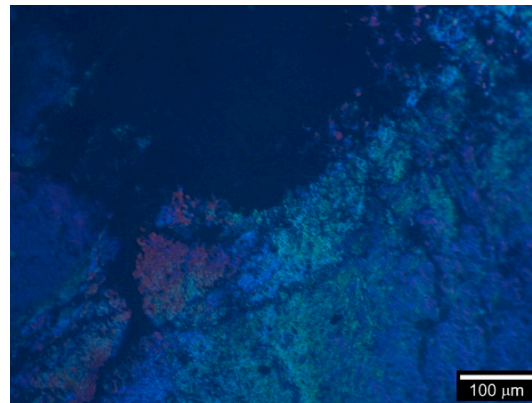


Figure 5. Circular polarized differential interference contrast optical microscopy (C-DIM) image of the emerald green part of C/PANI.

Figure 6a shows scanning electron microscopy (SEM) image of the C/PANI. The surface pebble structure is observed. Figure 6b displays electron probe micro analyzer (EPMA) observation results for carbon element of the C/PANI, indicating that pebbles on the surface contain high concentration of carbon. The EPMA profile of the carbon in the C/PANI confirmed distribution of the carbon in the sample. The carbon element in the sample and surface bulk structure may be the cause for the appearance of the surface color.

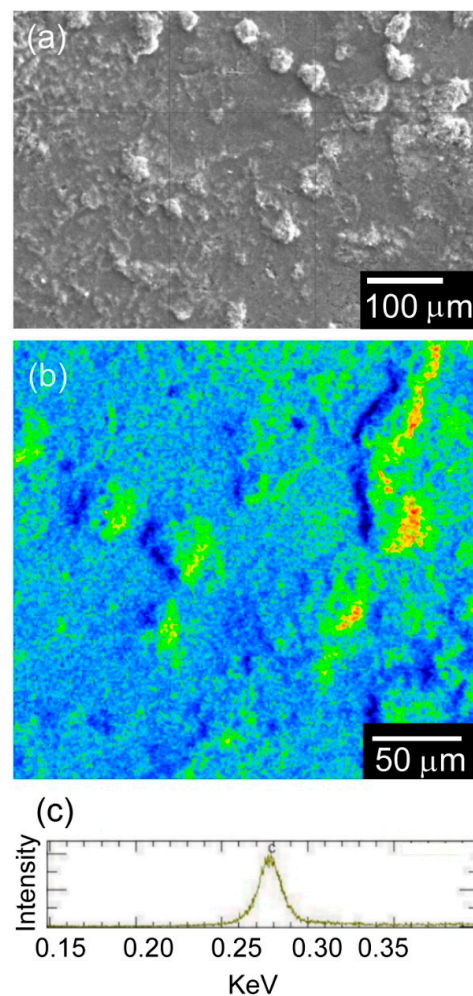


Figure 6. (a) Scanning electron microscopy image of C/PANI. (b) Electron probe micro analyzer (EPMA) results of carbon element for C/PANI. (c) The EPMA profile of carbon in C/PANI.

3.4. Synchrotron X-ray Diffraction

Synchrotron X-ray diffraction measurements for a pure PANI as a reference and C/PANI were carried out, as shown in Figure 7. The pure PANI showed diffractions at 13.8, 10.1, 6.1, 4.3, 3.5, 3.3, and 3.1 Å as typical diffractions of the emeraldine salt (PANI/ES). C/PANI exhibits diffractions at 10.7, 6.2, 4.4, 3.5, 3.4, 3.24, and 3.23 Å (inset of Figure 7). Especially, diffractions at 3.24 and 3.23 Å of C/PANI can be derived from carbon element in the C/PANI composite.

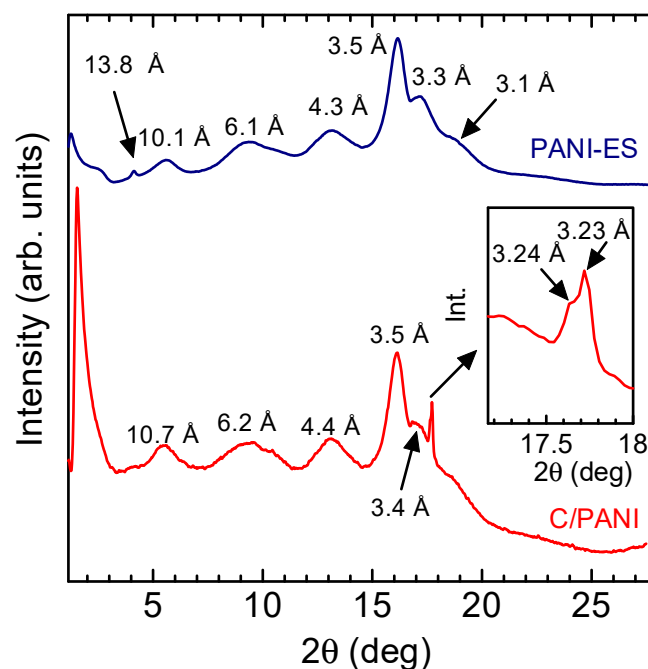


Figure 7. Synchrotron X-ray diffraction measurement results for pure PANI (PANI-ES) as a reference and C/PANI.

3.5. Electron Spin Resonance (ESR)

Figure 8 presents the ESR measurements for the C/PANI powder with a microwave power of 2.81 mW at 25 °C. The shape of the ESR signal differed from the symmetrical Lorentz-type. This may be due to the dielectric relaxation of carbon nanotubes and fullerenes in the PANI matrix. The signal intensity decreased with increasing microwave power (Figure 9). The resonance intensity changes with microwave power for the composite may lead to the development of devices that can detect low power microwaves. Electrical conductivity of C/PANI was 3.3 S/cm.

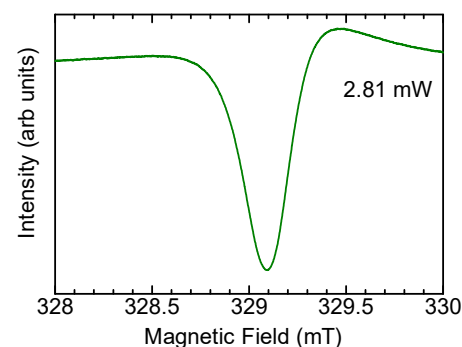


Figure 8. Electron spin resonance (ESR) measurement result for the C/PANI powder. Microwave power: 2.81 mW.

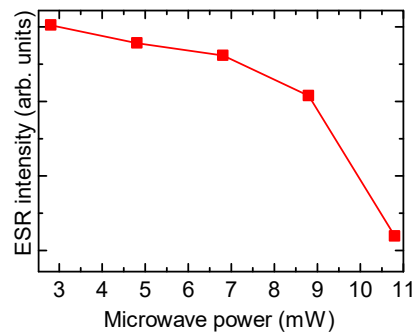


Figure 9. Change in the ESR intensity of C/PANI as a function of the microwave power.

3.6. Superconducting Quantum Interference Device Measurements

Figure 10a presents the χ vs. T and the χT vs. T plots for C/PANI, where χ is magnetic susceptibility. The magnetic behavior of C/PANI showed normal paramagnetism at low temperatures because χT vs. T in the Curie plot is constant. Figure 10b shows the magnification of the χ vs. T . The maximum of the χ value appeared at 265 K. The $1/\chi$ plots, as a function of temperature, exhibit a maximum at 105 K (Figure 7b, inset). This magnetic behavior was combined with the magnetic properties of PANI as Pauli's paramagnetism derived from polarons, the carbons, and electromagnetic interaction between PANI and the carbons.

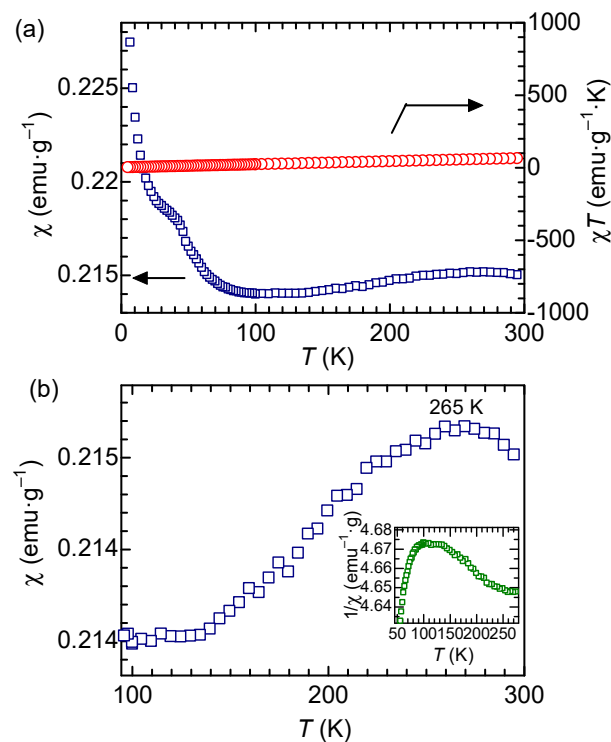


Figure 10. (a) χ vs. T and χT vs. T plots for C/PANI. (b) Magnification of χ vs. T ; inset shows $1/\chi$. χ : Magnetic susceptibility. T : Temperature.

3.7. I-V Character

Figure 11 displays current (I) as a function of applied voltage (E) of C/PANI. Increase of applied voltage to C/PANI increased current, indicating typical ohmic property, confirming electrical conducting function of C/PANI. Although the current is proportional to the voltage, the slight deviation from the linearity of the I - V (I - E) below -4 V may be caused by Joule heat.

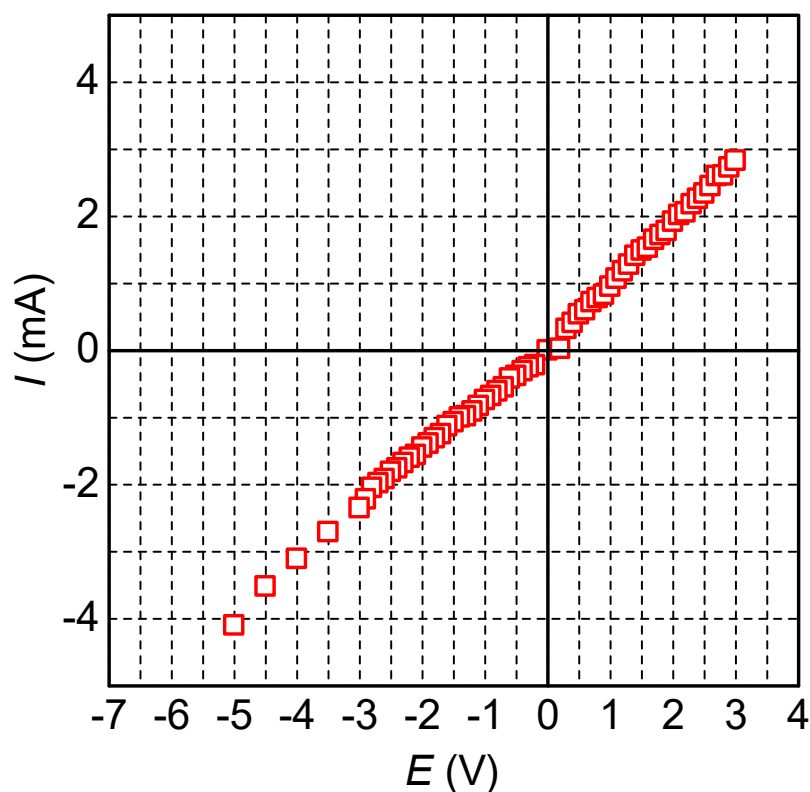


Figure 11. Current (I) as a function of applied voltage (E) of C/PANI.

4. Applications

Polymer blends consisting of PANI, carbon, and hydroxypropyl cellulose (HPC) or acryl resin were prepared. We previously reported facile synthesis of PANI in the presence of iodine in organic solvents [17,18]. The preparation of PANI in organic solvents can produce polymer plastic blends during the polymerization process of aniline. Further, addition of carbons in the polymerization reaction allows us to prepare C/PANI/plastics. Based on this concept, we prepared two plastic blends consisting of PANI, carbon, and HPC or acryl resin.

Synthesis of the HPC-based blends is simple. Aniline as a monomer (1 g), the carbons (1 g in a water solution), sulfuric acid (0.5 g), and HPC (5.5 g) were mixed in 5 mL of distilled water. Then, the solution was cooled to 0 °C, and stirred with a mechanical stirrer. APS (1 g) was added to the solution and the solution was stirred for 24 h. The solution was dried to obtain PANI, carbon, and HPC plastic blend (C/PANI/HPC).

Synthesis of the acryl resin-based blends was carried out by mixing aniline as a monomer (0.5 g), benzenesulfonic acid (1 g), iodine (0.03 g), acryl resin (1.8 g), the carbons (0.9 g, in a water solution) in 10 mL of chloroform. Then, the solution was cooled to 0 °C, and stirred with a mechanical stirrer. APS (1 g) was added to the solution and the solution was stirred for 24 h. The solution was dried to obtain the plastic consisting of PANI, carbon, and acryl resin (C/PANI/Acryl).

Figure 12 displays an optical microscopy image of C/PANI/HPC with transmission light at 25 °C, showing birefringence derived from liquid crystal form of the matrix HPC. Green color of the polymer blend is derived from the PANI emeraldine element.

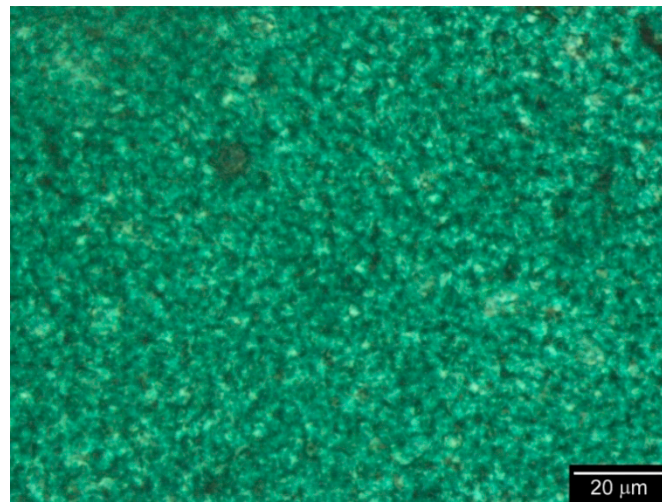


Figure 12. Optical microscopy image of PANI, C, and HPC blend plastic (C/PANI/HPC).

Figure 13 displays a circular polarized differential contrast interference optical microscopy image of C/PANI/Acryl with reflection light at 25 °C. A clear image of the carbons in the plastic blend was not observed because the fine sized carbons were dispersed in the blend. Black circles are bubbles of air in the sample with no birefringence.

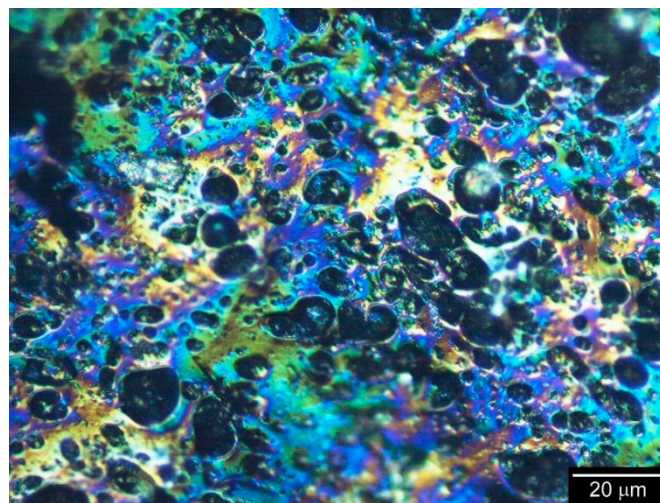


Figure 13. Polarizing optical microscopy image of PANI, C, and HPC plastic blend (C/PANI/Acryl).

Figure 14a displays IR spectra of the carbons, HPC, C/PANI/Acryl. The absorption band at 1118 cm^{-1} of C/PANI/HPC was derived from the absorption band of the HPC. The absorption of C/PANI/HPC at 1648 cm^{-1} was also observed for the carbons, indicating C/PANI/HPC had partly the same character of the carbons and the HPC. An absorption of carbons at 1392 cm^{-1} was also observable for C/PANI/acryl (Figure 14b). C/PANI/acryl had absorption band at 1134 cm^{-1} , which was observed for the acryl resin. The IR of C/PANI/acryl showed both characteristics of the carbons and acryl resin. The polymer blends had the absorption bands from the carbons and the matrix resins.

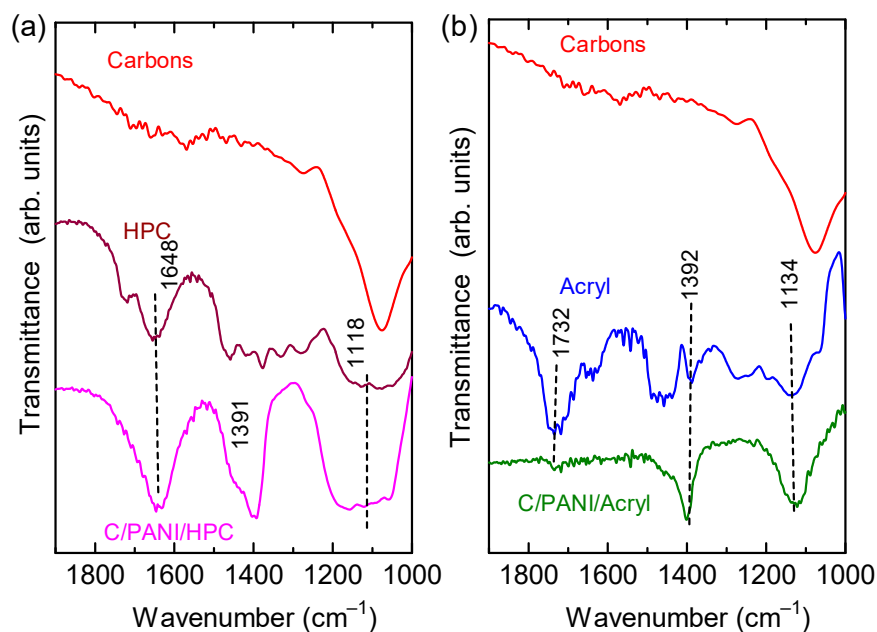


Figure 14. IR spectra of carbons, HPC, and C/PANI/HPC (a) and carbons, acryl resin, and C/PANI/acryl (b).

Electrical conductivities of C/PANI/HPC and C/PANI/Acryl were 8.3×10^{-3} S/cm and 5.2×10^{-5} S/cm, respectively, measured by the four-probe method, indicating these plastic blends had electrical conductivity. The plastics can be processed for making thin films and ingots for use for conducting vessels, packages, and wrapping items with electromagnetic shielding functions.

5. Conclusions

PANI was synthesized in the presence of the fullerene nanotubes (tubes@rice) to prepare C/PANI composites. The composite showed unique magnetic behavior, such as microwave power-dependent magnetic resonance as magnetic spin behavior and macroscopic paramagnetism with a maximum χ value at room temperature. Polymer blends consisting of PANI, C, and HPC or acryl resin having conducting polymer and carbon characters can be applied for electrical conducting plastics. The combination of conducting polymer and nano-carbon materials can produce new electro-magneto-active soft materials by forming a composite.

Author Contributions: Y.K. and H.G. synthesized polymer. H.G. synthesized polymer plastic blends. Y.K., R.M. and H.G. carried out the SQUID measurements. Y.K. and H.G. performed the ESR measurements. K.K. obtained the SEM and the EPMA data. T.Y. and R.K. obtained the synchrotron XRD data. H.G. conducted this project. H.G. found metallic emerald of the PANI. All authors have read and agreed to the published version of the manuscript.

Funding: This research was supported by the Japan Society for the Promotion of Science, Grants-in-Aid for Scientific Research (No. 20K05626).

Data Availability Statement: Not applicable.

Acknowledgments: We would like to thank the Open Facility, Research Facility Center for Science and Technology, and University of Tsukuba. Synchrotron XRD measurements were carried out at BL-8B beamline of the Photon Factory (PF), Institute of Materials Structure Science, KEK. The measurements were performed under the approval of the Photon Factory Program Advisory Committee (Proposal No. 2021G503).

Conflicts of Interest: The authors declare no conflict of interest.

References

1. Smith, B.; Monthieux, M.; Luzzi, D. Encapsulated C₆₀ in carbon nanotubes. *Nature* **1998**, *396*, 323–324. [[CrossRef](#)]
2. Shinohara, H. Exploring the inner space of carbon nanotubes. *Jpn. J. Appl. Phys.* **2018**, *57*, 020101. [[CrossRef](#)]
3. Service, R.F. Solid-State Physics: Nanotube ‘Peapods’ show electrifying promise. *Science* **2001**, *292*, 45. [[CrossRef](#)] [[PubMed](#)]
4. Chen, J.; Dong, J. Electronic properties of peapods: Effects of fullerene rotation and different types of tube. *J. Phys. Cond. Mat.* **2004**, *16*, 1401–1408. [[CrossRef](#)]
5. Sandeep, G.; Felix, B.; Alicja, B.; Maria, D.; Ronny, S.; Franziska, S.; Jürgen, T.; Thomas, G.; Ewa, B.-P.; Jamie, H.W.; et al. In situ observations of fullerene fusion and ejection in carbon nanotubes. *Nanoscale* **2010**, *2*, 2077–2079. [[CrossRef](#)]
6. Kausar, A. Carbon peapod encapsulating fullerene and inorganic nanoparticle toward polymeric nanocomposite: Tailored features and promises. *Poly. Plast. Technol. Mater.* **2022**, *61*, 1481–1502. [[CrossRef](#)]
7. Kausar, A. Fullerene nanowhisker nanocomposite—Current stance and high-tech opportunities. *Poly. Plast. Technol. Mater.* **2022**, *61*, 593–608. [[CrossRef](#)]
8. Wolfgang, K.M.; Jiménez, P.; Payne, N.O.; Shepherd, R.; Shepherd, R.L.; Castell, P.; Panhuis, M.I.H.; Benito, A.M. Nanofibrillar-Polyaniline/Carbon Nanotube Composites: Aqueous Dispersions and Films. *J. Nanosci. Nanotech.* **2009**, *9*, 6157–6163. [[CrossRef](#)]
9. Iwamori, R.; Sato, R.; Kuwabara, J.; Kanbara, T. Nonstoichiometric hydroarylation polyaddition for synthesis of pyrrole-based poly(arylenevinylene)s. *Polym. Chem.* **2022**, *13*, 379–382. [[CrossRef](#)]
10. Chen, X.; Ichige, A.; Chen, J.; Fukushima, I.; Kuwabara, J.; Kanbara, T. Facile Access to Conjugated Polymers under Aerobic Conditions via Pd-Catalyzed Direct Arylation and Aryl Amination Polycondensation. *Polymer* **2020**, *207*, 122927. [[CrossRef](#)]
11. Tamao, K.; Sumitani, K.; Kumada, M.J. Selective carbon-carbon bond formation by cross-coupling of Grignard reagents with organic halides. Catalysis by nickel-phosphine complexes. *J. Am. Chem. Soc.* **1972**, *94*, 4374. [[CrossRef](#)]
12. Komaba, K.; Goto, H. Soliton excitations in liquid crystal polyacetylene. *Mol. Cryst. Liq. Cryst.* **2020**, *703*, 69. [[CrossRef](#)]
13. Goto, H. Doping-Dedoping-Driven Optic Effect of π -Conjugated Polymers Prepared in Cholesteric-Liquid-Crystal Electrolytes. *Phys. Rev. Lett.* **2007**, *98*, 253901. [[CrossRef](#)] [[PubMed](#)]
14. MacDiarmid, A.G.; Chiang, J.C.; Richter, A.F.; Somasiri, N.L.D.; Epstein, A.J. Polyaniline: Synthesis and Characterization of the Emeraldine Oxidation State by Elemental Analysis. In *Conducting Polymers*; Alcácer, L., Ed.; Springer: Dordrecht, The Netherlands, 1987. [[CrossRef](#)]
15. Godovsky, D.Y.; Varfolomeev, A.E.; Zaretsky, D.F.; Chandrakanthi, N.R.L.; Kündig, A.; Wederc, C.; Caseri, W. Preparation of nanocomposites of polyaniline and inorganic semiconductors. *J. Mater. Chem.* **2001**, *11*, 2465–2469. [[CrossRef](#)]
16. Chatterjee, M.J.; Ghosh, A.; Mondal, A.; Banerjee, D. Polyaniline-single walled carbon nanotube composite—A photocatalyst to degrade rose bengal and methyl orange dyes under visible-light illumination. *RSC Adv.* **2017**, *7*, 36403–36415. [[CrossRef](#)]
17. Miyashita, R.; Goto, H. Preparation of polyaniline in organic liquid crystal solvent. *Mol. Cryst. Liq. Cryst.* **2021**, *738*, 1–7. [[CrossRef](#)]
18. Goto, H.; Komaba, K.; Yonehara, T.; Miyashita, R.; Kumai, R. Synthesis of polyaniline in organic solvents. *Polym.-Plast. Technol. Mater.* **2022**, *61*, 1593–1606. [[CrossRef](#)]